

Table-top soft x-ray microscope using laser-induced plasma from a pulsed gas jet

Matthias Müller,^{1,*} Tobias Mey,¹ Jürgen Niemeyer,² and Klaus Mann¹

¹Laser-Laboratorium Göttingen e.V., Hans-Adolf-Krebs-Weg 1, D-37077 Göttingen, Germany

²Department für Nutzpflanzenwissenschaften, Universität Göttingen, Carl-Sprengel-Weg 1, D-37075 Göttingen, Germany

*matthias.mueller@llg-ev.de

Abstract: An extremely compact soft x-ray microscope operating in the “water window” region at the wavelength $\lambda = 2.88$ nm is presented, making use of a long-term stable and nearly debris-free laser-induced plasma from a pulsed nitrogen gas jet target. The well characterized soft x-ray radiation is focused by an ellipsoidal grazing incidence condenser mirror. Imaging of a sample onto a CCD camera is achieved with a Fresnel zone plate using magnifications up to 500x. The spatial resolution of the recorded microscopic images is about 100 nm as demonstrated for a Siemens star test pattern.

©2014 Optical Society of America

OCIS codes: (180.7460) X-ray microscopy; (260.6048) Soft x-rays; (350.5400) Plasmas.

References and links

1. W. Meyer-Ilse, D. Hamamoto, A. Nair, S. A. Lelièvre, G. Denbeaux, L. Johnson, A. L. Pearson, D. Yager, M. A. Legros, and C. A. Larabell, “High resolution protein localization using soft x-ray microscopy,” *J. Microsc.* **201**(3), 395–403 (2001).
2. C. A. Larabell and M. A. Le Gros, “X-ray tomography generates 3-d reconstructions of the yeast, *Saccharomyces cerevisiae*, at 60-nm resolution,” *Mol. Biol. Cell* **15**(3), 957–962 (2004).
3. M. Juenger, V. Lamour, P. Monteiro, E. Gartner, and G. Denbeaux, “Direct observation of cement hydration by soft x-ray transmission microscopy,” *J. Mater. Sci. Lett.* **22**(19), 1335–1337 (2003).
4. G. Schneider, “Cryo x-ray microscopy with high spatial resolution in amplitude and phase contrast,” *Ultramicroscopy* **75**(2), 85–104 (1998).
5. D. Weiß, G. Schneider, B. Niemann, P. Guttman, D. Rudolph, and G. Schmahl, “Computed tomography of cryogenic biological specimens based on x-ray microscopic images,” *Ultramicroscopy* **84**(3-4), 185–197 (2000).
6. S. C. Myneni, J. T. Brown, G. A. Martinez, and W. Meyer-Ilse, “Imaging of humic substance macromolecular structures in water and soils,” *Science* **286**(5443), 1335–1337 (1999).
7. W. Chao, P. Fischer, T. Tyliczek, S. Rekawa, E. Anderson, and P. Naulleau, “Real space soft x-ray imaging at 10 nm spatial resolution,” *Opt. Express* **20**(9), 9777–9783 (2012).
8. S. Rehbein, P. Guttman, S. Werner, and G. Schneider, “Characterization of the resolving power and contrast transfer function of a transmission x-ray microscope with partially coherent illumination,” *Opt. Express* **20**(6), 5830–5839 (2012).
9. M. Berglund, L. Rymell, M. Peuker, T. Wilhein, and H. M. Hertz, “Compact water-window transmission x-ray microscopy,” *J. Microsc.* **197**(3), 268–273 (2000).
10. P. Jansson, U. Vogt, and H. Hertz, “Liquid-nitrogen-jet laser-plasma source for compact soft x-ray microscopy,” *Rev. Sci. Instrum.* **76**(4), 043503 (2005).
11. P. A. Takman, H. Stollberg, G. A. Johansson, A. Holmberg, M. Lindblom, and H. M. Hertz, “High-resolution compact x-ray microscopy,” *J. Microsc.* **226**(2), 175–181 (2007).
12. M. Benk, K. Bergmann, D. Schäfer, and T. Wilhein, “Compact soft x-ray microscope using a gas-discharge light source,” *Opt. Lett.* **33**(20), 2359–2361 (2008).
13. H. Legall, G. Blobel, H. Stiel, W. Sandner, C. Seim, P. Takman, D. H. Martz, M. Selin, U. Vogt, H. M. Hertz, D. Esser, H. Sipma, J. Luttmann, M. Höfer, H. D. Hoffmann, S. Yulin, T. Feigl, S. Rehbein, P. Guttman, G. Schneider, U. Wiesemann, M. Wirtz, and W. Dietsch, “Compact x-ray microscope for the water window based on a high brightness laser plasma source,” *Opt. Express* **20**(16), 18362–18369 (2012).
14. J. Allain, A. Hassanein, M. Allain, B. Heuser, M. Nieto, C. Crobak, D. Rokusek, and B. Rice, “Xe⁺ irradiation effects on multilayer thin-film optical surfaces in EUV lithography,” *Nucl. Instrum. Methods Phys. Res. B* **242**(1-2), 520–522 (2005).
15. H. Fiedorowicz, A. Bartnik, Z. Patron, and P. Piotr, “X-ray emission from laser-irradiated gas puff targets,” *Appl. Phys. Lett.* **62**(22), 2778–2780 (1993).

16. S. Kranzusch and K. Mann, "Spectral characterization of EUV radiation emitted from a laser-irradiated gas puff target," *Opt. Commun.* **200**(1-6), 223–230 (2001).
 17. F. Barkusky, C. Peth, A. Bayer, and K. Mann, "Direct photo-etching of poly(methyl methacrylate) using focused extreme ultraviolet radiation from a table-top laser-induced plasma source," *J. Appl. Phys.* **101**(12), 124908 (2007).
 18. C. Peth, F. Barkusky, and K. Mann, "Near-edge x-ray absorption fine structure measurements using a laboratory-scale XUV source," *J. Phys. D Appl. Phys.* **41**(10), 105202 (2008).
 19. A. Bartnik, H. Fiedorowicz, R. Jarocki, J. Kostecki, A. Szczurek, and M. Szczurek, "Ablation and surface modifications of PMMA using a laser-plasma EUV source," *Appl. Phys. B* **96**(4), 727–730 (2009).
 20. G. Kubiak and M. Richardson, US Patent 5,577,092 (1996).
 21. H. Fiedorowicz, A. Bartnik, H. Daido, I. Choi, M. Suzuki, and S. Yamagami, "Strong extreme ultraviolet emission from a double-stream xenon/helium gas puff target irradiated with a Nd:YAG laser," *Opt. Commun.* **184**(1-4), 161–167 (2000).
 22. T. Mey, M. Rein, P. Großmann, and K. Mann, "Brilliance improvement of laser-produced soft x-ray plasma by a barrel shock," *New J. Phys.* **14**(7), 073045 (2012).
 23. S. Kranzusch, C. Peth, and K. Mann, "Spatial characterization of extreme ultraviolet plasmas generated by laser excitation of xenon gas targets," *Rev. Sci. Instrum.* **74**(2), 969–974 (2003).
 24. A. Bayer, F. Barkusky, S. Döring, P. Großmann, and K. Mann, "Applications of compact laser-driven EUV/XUV plasma sources," *X-Ray Opt. Instrum.* **2010**, 1–9 (2010).
 25. D. Proch and T. Trickl, "A high-intensity multi-purpose piezoelectric pulsed molecular beam source," *Rev. Sci. Instrum.* **60**(4), 713–716 (1989).
 26. M. Müller, F. C. Köhl, P. Großmann, P. Vrba, and K. Mann, "Emission properties of ns and ps laser-induced soft x-ray sources using pulsed gas jets," *Opt. Express* **21**(10), 12831–12842 (2013).
 27. B. L. Henke, E. M. Gullikson, and J. C. Davis, "X-Ray Interactions: Photoabsorption, Scattering, Transmission, and Reflection at $E = 50\text{--}30,000$ eV, $Z = 1\text{--}92$," *At. Data Nucl. Data Tables* **54**(2), 181–342 (1993).
 28. G. Cox, *Optical Imaging Techniques in Cell Biology* (CRC Press, 2012).
 29. M. Diehl, *Abbildungseigenschaften eines Röntgenmikroskops mit gepulster Plasmaquelle* (PhD thesis, University Göttingen, Shaker, 1994).
-

1. Introduction

Benefitting from the high absorption contrast between carbon and oxygen, transmission x-ray microscopy in the spectral range of the "water window" ($\lambda = 2.3 - 4.4$ nm) has been proven to be an extremely useful tool for the investigation of biological and mineralogical samples, accomplishing, e.g., tomographic studies of cryogenic cells [1–5] and spectromicroscopic analysis of soils, making use of the inherent element-specific contrast [6]. Using Fresnel zone plates as highly magnifying objectives spatial resolutions in the range of 10 nm have been achieved [7, 8]. However, owing to the necessary high photon flux of short wavelength radiation, until now, such studies are almost exclusively conducted at synchrotron sources.

In order to overcome this limitation there are ongoing efforts to employ also lab-scale sources based on laser-produced or gas discharge plasmas for soft x-ray microscopy. Considerable progress has already been achieved in this field [9–13]. For instance, Legall et al. [13] have recently described a system in which a laser plasma is generated in a liquid nitrogen cryo jet, making use of a master oscillator power amplifier (MOPA) laser that generates average powers of up to 130 W at sub-ns pulse durations. Micrographs of impressive quality with a resolution of several 10 nm, acquired at moderate exposure times, have been presented.

Notwithstanding these achievements, there is definitely still the need for further compaction and simplification of lab-scale soft x-ray microscopes in order to pave the way for their wider dissemination. Long-term stability and ease of operation are major issues in this context. In particular, a major problem of laser-produced and especially gas discharge plasma sources is the nearly inevitable generation of debris particles, which can severely damage optical elements in relatively close vicinity to the plasma, especially condenser mirrors [14]. Regarding laser-produced plasma sources, alternatives to solid or liquid jet target concepts should be considered in order to reduce or totally avoid optics degradation from debris. The operation of liquid jet targets requires also considerable experimental and technical effort including large pumping powers and liquid nitrogen cooling, impeding the development of compact devices.

Such inconveniences can be overcome by the use of short-pulsed gaseous targets, which enable the construction of rather clean, compact and long-term stable soft x-ray sources [15, 16]. Such devices have already been successfully applied in various fields, ranging from material ablation and structuring to absorption spectroscopy [17–19], although their photon yields and peak brilliances are definitely smaller, as the plasma size increases to several hundreds of μm due to the lower particle density [15]. However, progress in the optimization of gaseous plasma sources has been achieved by using cluster beam targets [20], double-stream gas puff targets [21], or by forming supersonic jets in combination with a barrel shock [22], all leading to smaller and brighter plasmas due to locally enhanced particle densities.

In the work presented here we demonstrate that soft x-ray microscopy in the “water window” range can be accomplished by an extremely compact and long-term stable setup, using a standard Q-switch ns laser and a pulsed gas jet as inherently debris-free target for plasma generation. Along with a description of the new microscope operating with monochromatic radiation from He-like nitrogen at a wavelength of 2.88 nm first micrographs from various samples are presented.

2. Experimental

The setup of the table-top soft x-ray microscope is depicted in Fig. 1.

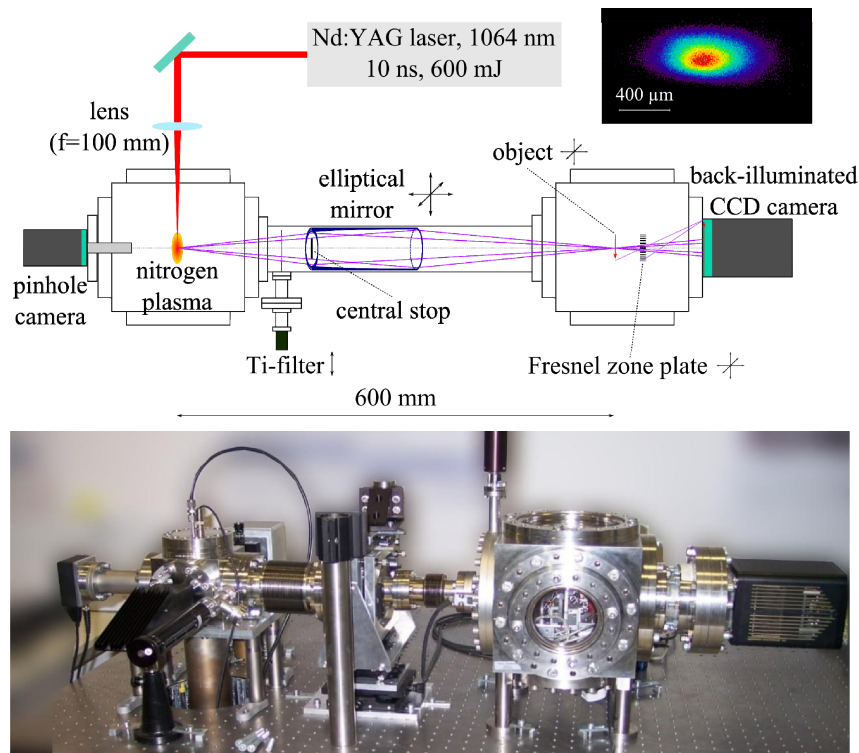


Fig. 1. Schematic drawing (top) and photograph (bottom) of the table-top soft x-ray microscope (cf. text). The inset shows a pinhole camera image of the laser-induced nitrogen plasma averaged over 10 pulses recorded for the emission wavelength of 2.88 nm.

It consists basically of a laser-induced plasma source, an ellipsoidal condenser mirror, a Fresnel zone plate objective, and a back-illuminated CCD camera sensitive for soft x-ray radiation. Due to the high absorption cross-section of soft x-rays with matter, the experiments are performed in a vacuum system with a base pressure of $1 \cdot 10^{-6}$ mbar.

The laser-induced plasma source has been described in detail elsewhere [23, 24]. It is based on a gas target and a Nd:YAG laser system (Quantel, wavelength 1064 nm, pulse

energy 600 mJ, pulse duration 10 ns). The pulsed gas jet used as laser target is created by a fast valve (Proch-Trickl setup [25]), consisting of a piezo disk translator (Physik-Instrumente, P-286.72) to generate short gas pulses ($t_{\text{open}} = 900 \mu\text{s}$). It allows for a pressure of about $5 \cdot 10^{-3}$ mbar during operation (repetition rate 5 Hz, gas backing pressure $p = 20$ bar). The gas jet is formed by a conically diverging nozzle (300 μm to 550 μm diameter). The laser beam is focused by a lens with focal length $f = 100$ mm onto a nitrogen gas jet. The radiation emitted from the nitrogen plasma is filtered by a titanium (Ti) filter (thickness 200 nm) to block out-of-band radiation, such as visible light or scattered laser radiation. Furthermore, radiation below the Ti L-edge ($\lambda = 2.7$ nm) is also blocked, ensuring monochromatic irradiation of the sample at $\lambda = 2.88$ nm wavelength. Figure 2 shows the emission spectra of nitrogen in the wavelength range from 1.5 nm to 3.5 nm measured with Al and Ti filters, respectively [26].

The spatial distribution of the nitrogen plasma is monitored by a pinhole camera (pinhole diameter 50 μm) utilizing a CCD chip (Sony ICX285, $6.45 \cdot 6.45 \mu\text{m}^2$ pixel size, $1280 \cdot 1024$ pixels) sensitized to the soft x-ray spectral range by a phosphor coating (cf. Figure 1). The pinhole camera is also equipped with a Ti filter ensuring registration of the plasma in the “water window” range only; the nitrogen plasma size at $\lambda = 2.88$ nm is measured to be $0.44 \cdot 0.24 \text{ mm}^2$ (FWHM).

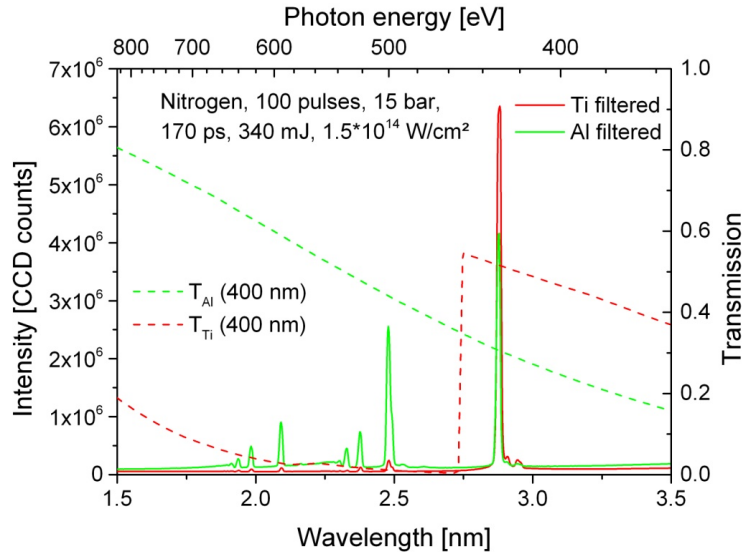


Fig. 2. Emission spectra of nitrogen in the wavelength range from 1.5 nm to 3.5 nm measured with Al and Ti filters, respectively. Transmission data of both filters are taken from CXRO [27].

The soft x-ray radiation from the nitrogen plasma is collected and focused by an ellipsoidal, axisymmetric nickel coated condenser mirror (Rigaku, Inc., focal length 300 mm, mirror length 100 mm) into the object plane. The condenser has an entrance numerical aperture of $NA_{C_in} = 0.071$ and an exit numerical aperture of $NA_{C_out} = 0.044$, respectively, resulting in a magnification of the focus size by a factor of $NA_{C_in}/NA_{C_out} = 1.6$. A Fresnel zone plate objective (ZonePlates Ltd., 190 μm diameter, minimum zone width $dr_n = 30$ nm, number of zones 1580) images the sample onto a soft x-ray sensitive CCD camera (Roper Scientific, back-thinned back-illuminated, $13 \cdot 13 \mu\text{m}^2$ pixel size, $1024 \cdot 1024$ pixels) using magnifications up to 500x. The numerical aperture of the Fresnel zone plate is $NA_{FZP} = 0.048$, thus nearly matching the exit numerical aperture of the condenser ($NA_{C_out}/NA_{FZP} = 0.92$). Both sample and Fresnel zone plate are mounted on motorized three-axis translation stages (mechOnics). Since the depth of focus of the Fresnel zone plate is only $\pm 0.62 \mu\text{m}$ at 2.88 nm,

the zone plate is moved along the optical axis with a step size of 1 μm in order to obtain the image with the highest resolution. The CCD camera is cooled down to $-40\text{ }^\circ\text{C}$ to reduce its intrinsic thermal noise during image acquisition. Additionally, a background map was subtracted from all micrographs to account for systematic non-uniformities of the CCD camera.

3. Results and discussion

Before installation of the Fresnel zone plate, the adjustment of the grazing incidence condenser mirror was optimized by the measurement of intensity profiles at various positions along the optical axis (z -axis), utilizing both the phosphor coated CCD chip (as in pinhole camera) and the back-illuminated CCD camera. Figure 3 displays the results of these measurements for different camera positions. To record the spatial distribution in the focus of the ellipsoid without overexposure of the camera the radiation was attenuated with a polypropylene foil of 4 μm thickness (transmission 0.2% at $\lambda = 2.88\text{ nm}$ [27]). A Gaussian-like spatial profile with a diameter of $d_x = (430 \pm 10)\text{ }\mu\text{m}$ and $d_y = (420 \pm 10)\text{ }\mu\text{m}$ (FWHM) is registered for the focal plane ($z = 0$), representing the object plane of the soft x-ray microscope.

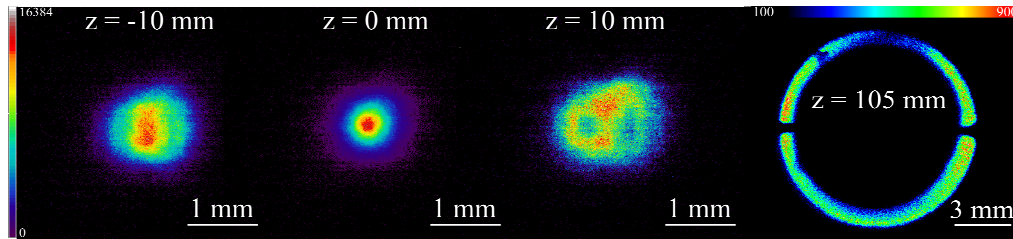


Fig. 3. Spatial intensity distribution of soft x-ray radiation at $\lambda = 2.88\text{ nm}$ for different positions along the optical axis behind the ellipsoidal condenser mirror; the minimum spot diameter at $z = 0\text{ mm}$ (object plane) is $d_x = (430 \pm 10)\text{ }\mu\text{m}$ and $d_y = (420 \pm 10)\text{ }\mu\text{m}$, respectively. For a better view of the spatial profiles the intensities at $z = -10\text{ mm}$ and $z = 10\text{ mm}$ were enhanced by a factor of 2. The image at $z = 105\text{ mm}$ was taken with the back-illuminated CCD camera (see text).

Measurement of the pulse energy in the focal spot is conducted with a calibrated XUV photo-diode (IRD AXUV100) with Ti filter in place. Taking into account the fractional energy seen by the Fresnel zone plate (diameter 190 μm), the single pulse energy density in the object plane is determined to be $(0.040 \pm 0.005)\text{ mJ/cm}^2$ corresponding to about $5.8 \cdot 10^3$ photons/ μm^2 per pulse.

In order to assess the imaging performance of the microscope over the full field of view (FOV), a Siemens star test pattern (NTT-AT, model ATN/XRESO-50, 200 nm Ta on Ru(50 nm)/SiN(200 nm) membrane) was imaged. Figure 4 shows a corresponding micrograph, indicating an almost uniform illumination over a field of view of $\approx 10\text{ }\mu\text{m}$ (cf. Figure 4 inset). Structures with a size of $\approx 100\text{ nm}$ are resolved in all directions. Without sample the detector is illuminated with ≈ 0.8 photons/s/pixel (size 26 nm, magnification 500x). These photon numbers indicate a zone plate diffraction efficiency of about 4%, which is consistent with the specification provided by the manufacturer and is comparable to the results of Legall et al. [13], who have reported ≈ 12 photons/s/pixel for the same pixel size and a 20 times higher average laser power.

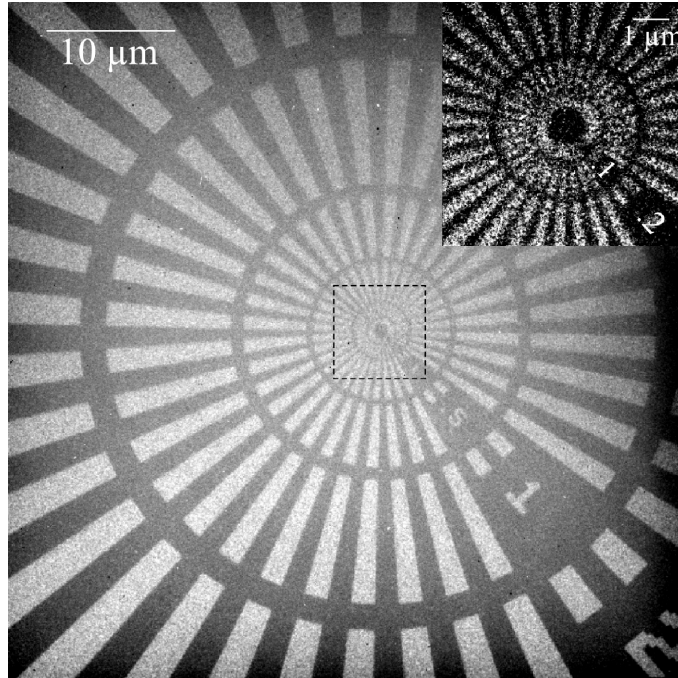


Fig. 4. Soft x-ray micrograph of Siemens star recorded with a pixel element size of $52 \times 52 \text{ nm}^2$ (magnification $M = 250$) using 18000 pulses (60 min). The inset showing the central part of the Siemens star is recorded separately at a higher magnification of 500 (pixel element size $26 \times 26 \text{ μm}^2$) using 36000 pulses (120 min).

Furthermore, geo-colloids collected from a water sample (Main river / central Germany) and suspended on a Si_3N_4 membrane (Silson, thickness 200 nm) were investigated at a magnification of 500, showing micro-structured as well as irregular particles (cf. Figure 5). The necklace-like structure visible in the lower part of the micrograph is supposed to stem from biological debris material. The spacing of the regularly arranged isolated “holes” is approximately 215 nm, indicating the high resolution capacity of the table-top soft x-ray microscope.

The maximal resolution of the described microscope given by the Fresnel zone plate is $\delta = 1.22 \cdot d r_n \approx 37 \text{ nm}$, assuming incoherent illumination. The discrepancy between this theoretical resolution and the obtained value of 100 nm can be explained by several factors: First of all, due to the digitization of the microscopic images (effective camera pixel size 26 nm at 500x) the achievable resolution is reduced to $2.3 \cdot 26 \text{ nm} = 60 \text{ nm}$ according to the Nyquist-Shannon sampling theorem [28]. Secondly, the obviously still rather low signal-to-noise ratio ($S/N \approx 9$) of the recorded micrographs results in a low image contrast which clearly reduces the spatial resolution. Calculations of the degree of coherence considering the hollow cone illumination of the condenser mirror show that effects of partial coherence must be considered for structures smaller than 110 nm [29], reducing the image contrast as well. Moreover, small vibrations as well as long-term thermal drifts of the optical setup may decrease the apparent resolution of the microscope, especially regarding the long exposure times (up to 120 min). In addition, small angular tilts of both Fresnel zone plate and sample might adversely influence the imaging performance. Nevertheless, the spatial resolution is relatively close to the maximal one.



Fig. 5. Soft x-ray microscopic image of geo-colloids taken from the Main River (18000 pulses, 60 min, pixel element size $26 \times 26 \text{ nm}^2$).

4. Conclusion and outlook

In this paper we have demonstrated the feasibility of a table-top soft x-ray microscope operating at a wavelength of 2.88 nm. It is based on an almost debris-free, long-term stable laser plasma produced in a gaseous target. Currently structures of about 100 nm in size are already detectable, being limited, among other factors, by the low signal-to-noise ratio due to the relatively low brilliance of the plasma. However, the presented system offers various opportunities for scalability of the photon flux, which have already been separately investigated in the past. First of all, lasers of higher repetition rate (average power) and / or shorter pulses can be employed. Recently it has been shown that, due to the higher degree of excitation, the use of ps laser pulses of the same energy as the currently employed ns pulses can boost the brightness of the plasma by more than a factor of 10 in the “water window” range [26]. Moreover, higher particle densities by use of either higher gas pressures or the barrel shock approach can increase the brilliance of the laser plasma by at least one order of magnitude [22].

Such improvements will be incorporated into the system in the future in order to reduce the exposure times for recording of micrographs, thereby maintaining the compactness of the microscope and especially the inherent cleanliness of the soft x-ray source.

Acknowledgment

Financial support by the “Deutsche Forschungsgemeinschaft” within “Sonderforschungsbereich 755” “Nanoscale Photonic Imaging” (Project C4) is gratefully acknowledged. The authors like to thank T. Salditt (Univ. Göttingen) for stimulating discussions.